# Electronic Supplementary Information

*for*

# Polymer Electron Donor based on Isoindigo Unit Bearing Branched Oligo(Ethylene Glycol) Side Chains for Polymer Solar Cells

*Xingxing Chen,*[a,b] *Zijian Zhang,*[a,b] *Jun Liu**[a] *and Lixiang Wang**[a]

[a]*State Key Laboratory of Polymer Physics and Chemistry, Changchun Institute of Applied Chemistry, Chinese Academy of Sciences, Changchun 130022, P. R. China.*
[b]*University of Chinese Academy of Sciences, Beijing 100049, P. R. China.*
*Email: liujun@ciac.ac.cn, lixiang@ciac.ac.cn*

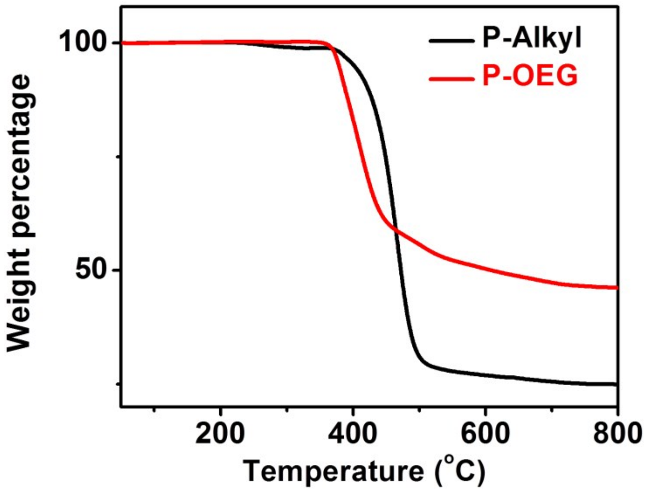

**Fig. S1** TGA curves of the two polymers. The two polymers show good thermal stability with decomposition temperatures ($T_d$) at 5% weight loss of 402 $^oC$ for P-Alkyl, 379 $^oC$ for P-OEG.

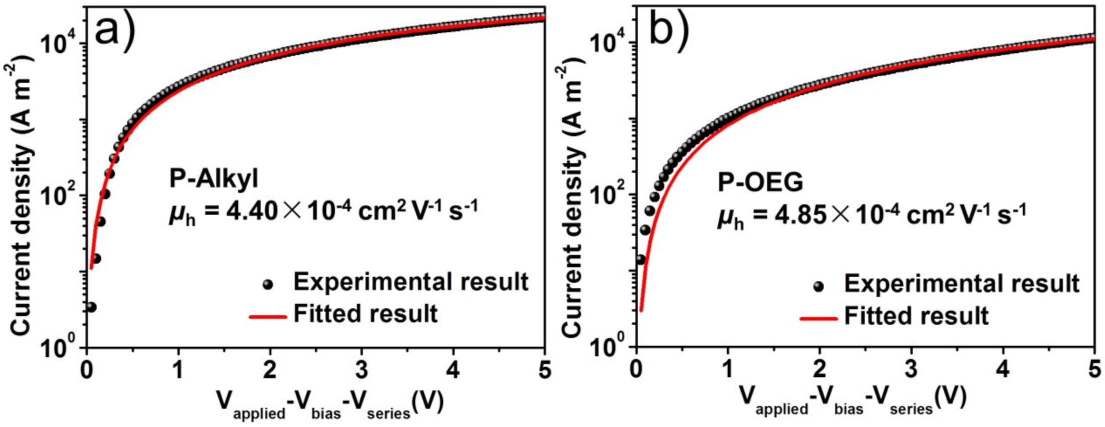

**Fig. S2** Current density-voltage (*J-V*) curves and space-charge-limited current (SCLC) fittings of the hole-only devices of the two polymers.

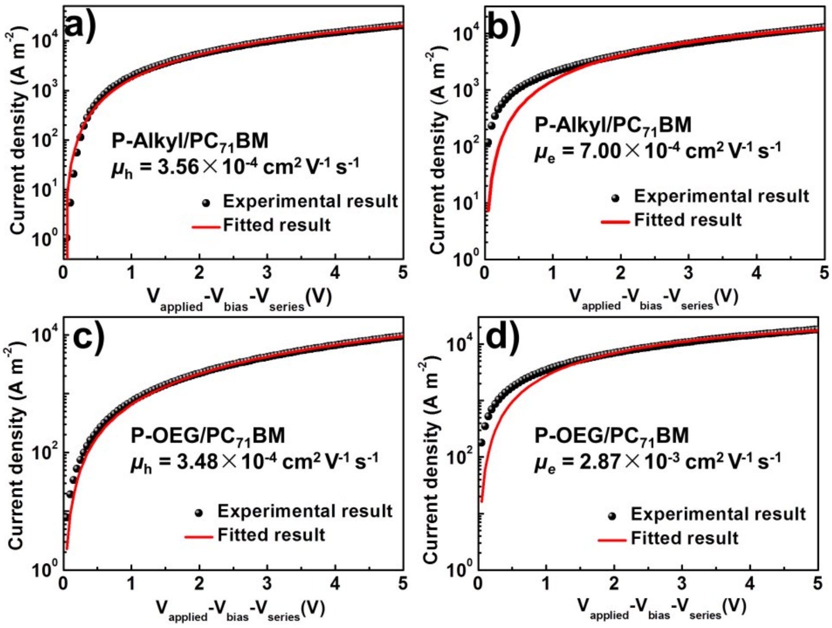

**Fig. S3** Current density-voltage (*J-V*) curves and space-charge-limited current (SCLC) fittings of the hole-only devices and the electron-only devices based on the blend films of P-Alkyl/PC$_{71}$BM and P-OEG/PC$_{71}$BM processed from CB solutions with 1 vol% and 3 vol% DIO, respectively.

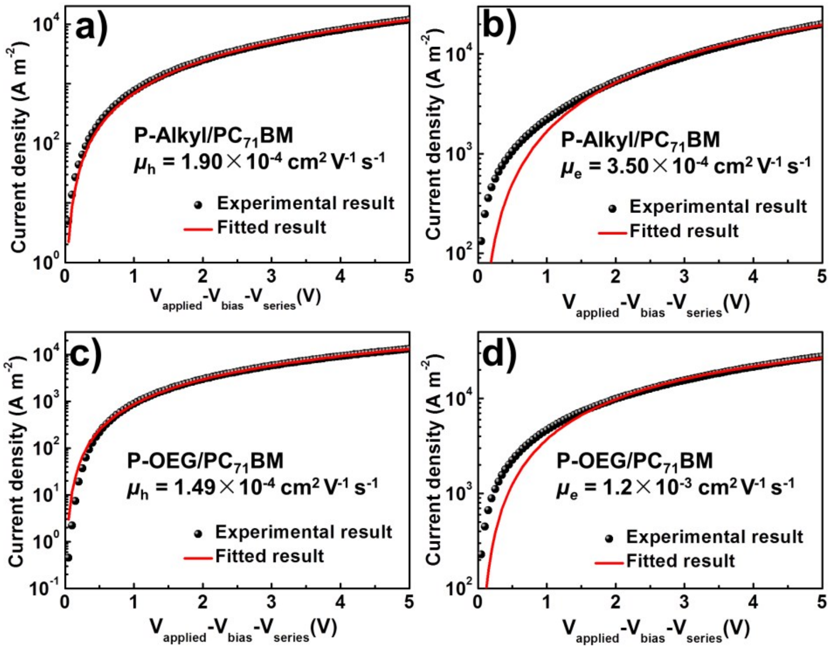

**Fig. S4** Current density-voltage (*J-V*) curves and space-charge-limited current (SCLC) fittings of the hole-only devices and the electron-only devices based on the blend films of P-Alkyl/$PC_{71}BM$ and P-OEG/$PC_{71}BM$ processed from CB solutions without DIO.

**Table S1** Summary of hole and electron mobility of the P-Alkyl/$PC_{71}BM$ and P-OEG/$PC_{71}BM$ blend films spin-coated without or with DIO.

| Active Layer | DIO (v/v%) | $\mu_h$ (cm$^2$ V$^{-1}$ s$^{-1}$) | $\mu_e$ (cm$^2$ V$^{-1}$ s$^{-1}$) | $\mu_h/\mu_e$ |
|---|---|---|---|---|
| P-Alkyl:$PC_{71}BM$ | 0 | $1.90\times10^{-4}$ | $3.50\times10^{-4}$ | 1/2 |
| | 3.0 | $3.56\times10^{-4}$ | $7.00\times10^{-4}$ | 1/2 |
| P-OEG:$PC_{71}BM$ | 0 | $1.49\times10^{-4}$ | $1.20\times10^{-3}$ | 1/8 |
| | 1.0 | $3.48\times10^{-4}$ | $2.87\times10^{-3}$ | 1/8 |

The charge mobilities of the two polymers were measured using space-charge-limited current (SCLC) method. The mobility was obtained by fitting the *J-V* curves near quadratic region according to the modified Mott-Gurney equation:

$$J = \frac{9}{8}\varepsilon_r\varepsilon_0\mu\frac{V^2}{L^3}\exp(0.89\beta\frac{\sqrt{V}}{\sqrt{L}})$$

where $J$ is the current density, $\varepsilon_0$ is vacuum permittivity, $\varepsilon_r$ is the relative permittivity, $\mu$ is the zero-field mobility, $V$ is the potential across the device ($V = V_{\text{applied}}-V_{\text{bias}}-V_{\text{series}}$), $L$ is the thickness of active layer, and $\beta$ is the field-activation factor. The series and contact resistance ($V_{\text{series}}$) of the device (10-20 Ω) were measured using blank device of ITO/PEIE/Ca/Al or ITO/PEDOT:PSS/$MoO_3$/Ag. The hole-only devices structure: ITO/PEDOT:PSS/polymers (polymer:$PC_{71}BM$)/$MoO_3$/Ag. The electron-only devices structure: ITO/PEIE/Active layer/Ca/Al

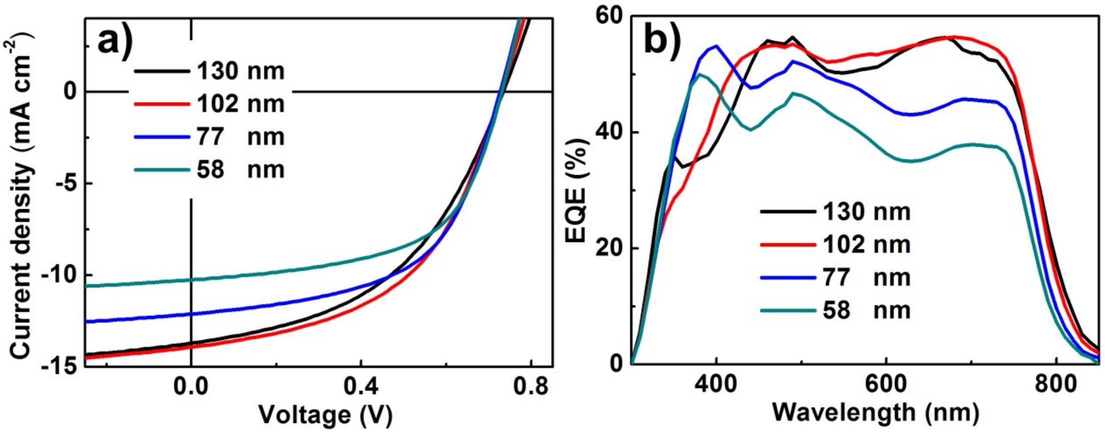

**Fig. S5** a) *J-V* and b) EQE curves of the PSC devices based on P-OEG/PC$_{71}$BM active layer processed from CB solution with 1 vol% DIO with different thickness.

**Table S2** Characteristics of the PSC devices based on the P-OEG/PC$_{71}$BM blend processed from CB solutions with 1 vol% DIO with different thickness.

| Thickness (nm) | $V_{OC}$ (V) | $J_{SC}$ (mA cm$^{-2}$) | FF (%) | PCE (%) | Rs (Ω cm$^{-2}$) | Rsh (Ω cm$^{-2}$) |
|---|---|---|---|---|---|---|
| 130 | 0.73 | 13.70 | 46.90 | 4.69 | 17 | 396 |
| 102 | 0.73 | 13.92 | 50.20 | 5.10 | 14 | 406 |
| 77 | 0.73 | 12.10 | 55.46 | 4.90 | 12 | 616 |
| 58 | 0.73 | 10.25 | 58.05 | 4.35 | 11 | 476 |

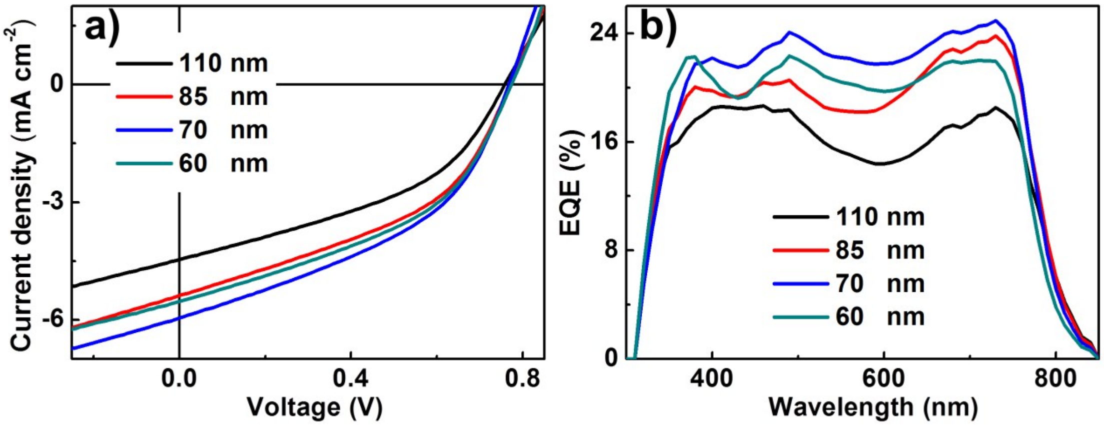

**Fig. S6** a) *J-V* and b) EQE curves of the PSC devices based on P-OEG/PC$_{71}$BM active layer processed from CB solution without DIO with different thickness.

**Table S3** Characteristics of the PSC devices based on the P-OEG/PC$_{71}$BM blend processed from CB solution without DIO with different thickness.

| Thickness (nm) | $V_{OC}$ (V) | $J_{SC}$ (mA cm$^{-2}$) | FF (%) | PCE (%) | Rs (Ω cm$^{-2}$) | Rsh (Ω cm$^{-2}$) |
|---|---|---|---|---|---|---|
| 110 | 0.76 | 4.46 | 42.00 | 1.43 | 50 | 381 |
| 85 | 0.77 | 5.39 | 42.20 | 1.75 | 39 | 279 |
| 70 | 0.77 | 5.95 | 42.80 | 1.96 | 32 | 259 |
| 60 | 0.77 | 5.38 | 43.75 | 1.81 | 39 | 351 |

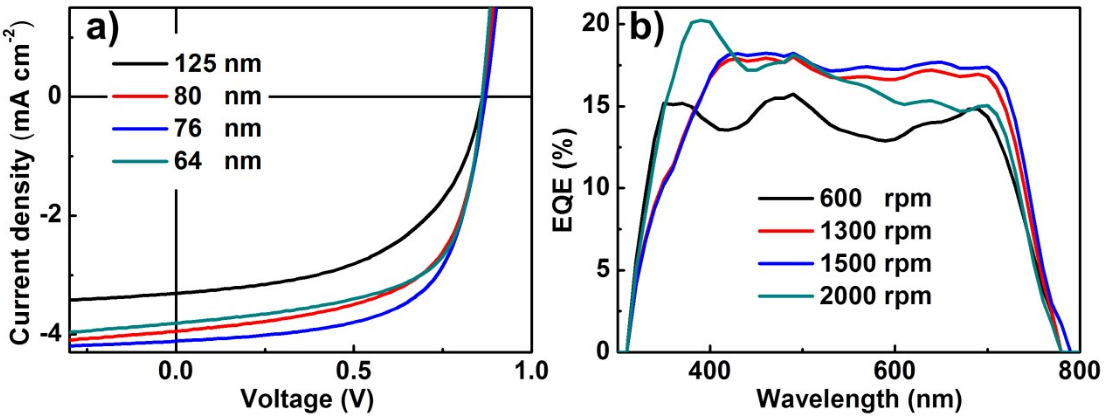

**Fig. S7** a) *J*-*V* and b) EQE curves of the PSC devices based on P-Alkyl/PC$_{71}$BM active layer processed from CB solution with 3 vol% DIO with different thickness.

**Table S4** Characteristics of the PSC devices based on the P-Alkyl/PC$_{71}$BM blend processed from CB solutions with 3 vol% DIO with different thickness.

| Thickness (nm) | $V_{OC}$ (V) | $J_{SC}$ (mA cm$^{-2}$) | FF (%) | PCE (%) | Rs (Ω cm$^{-2}$) | Rsh (Ω cm$^{-2}$) |
|---|---|---|---|---|---|---|
| 125 | 0.86 | 3.31 | 53.31 | 1.52 | 29 | 2730 |
| 80 | 0.87 | 3.96 | 60.33 | 2.08 | 19 | 1248 |
| 76 | 0.87 | 4.11 | 63.40 | 2.30 | 23 | 2357 |
| 64 | 0.86 | 3.79 | 63.45 | 2.07 | 17 | 3929 |

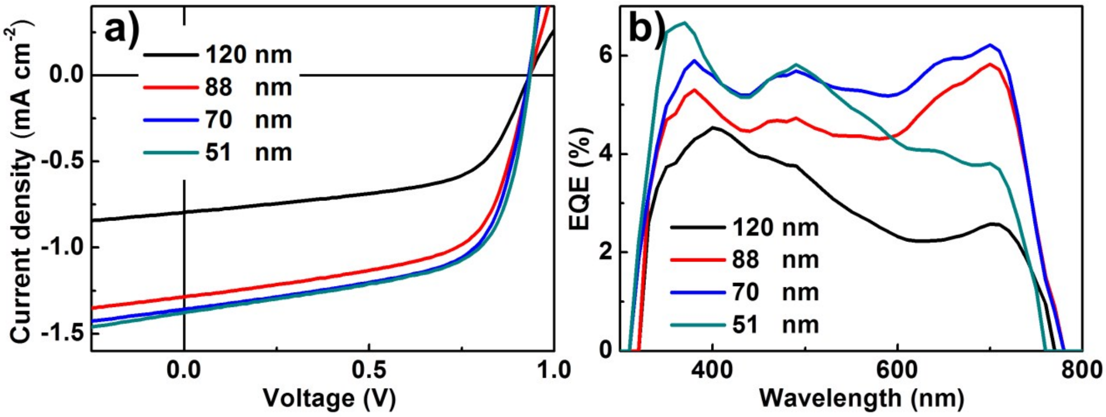

**Fig. S8** a) *J-V* and b) EQE curves of the PSC devices based on P-Alkyl/PC$_{71}$BM active layer processed from CB solution without DIO with different thickness.

**Table S5** Characteristics of the PSC devices based on the P-Alkyl/PC$_{71}$BM blend processed from CB solutions with 3 vol% DIO with different thickness.

| Thickness (nm) | $V_{OC}$ (V) | $J_{SC}$ (mA cm$^{-2}$) | FF (%) | PCE (%) | Rs (Ω cm$^{-2}$) | Rsh (Ω cm$^{-2}$) |
|---|---|---|---|---|---|---|
| 120 | 0.93 | 0.71 | 59.05 | 0.39 | 206 | 4900 |
| 88 | 0.93 | 1.16 | 61.74 | 0.67 | 114 | 3743 |
| 70 | 0.93 | 1.36 | 62.80 | 0.79 | 76 | 3421 |
| 51 | 0.93 | 1.09 | 62.97 | 0.64 | 51 | 2251 |

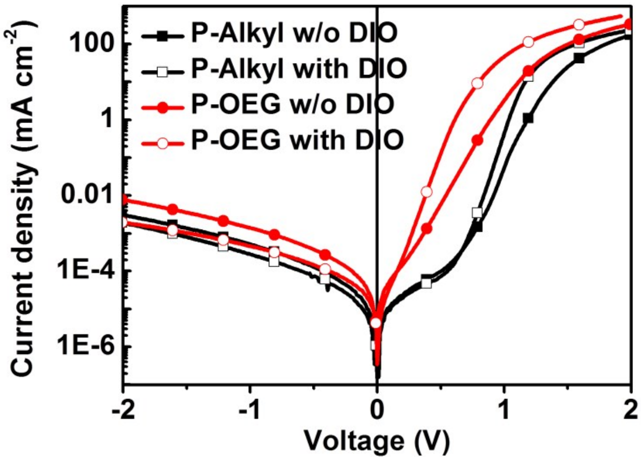

**Fig. S9** *J-V* curves of the PSC devices in dark based on P-Alkyl/PC$_{71}$BM and P-OEG/PC$_{71}$BM active layers spin-coated from CB solutions with and without DIO.

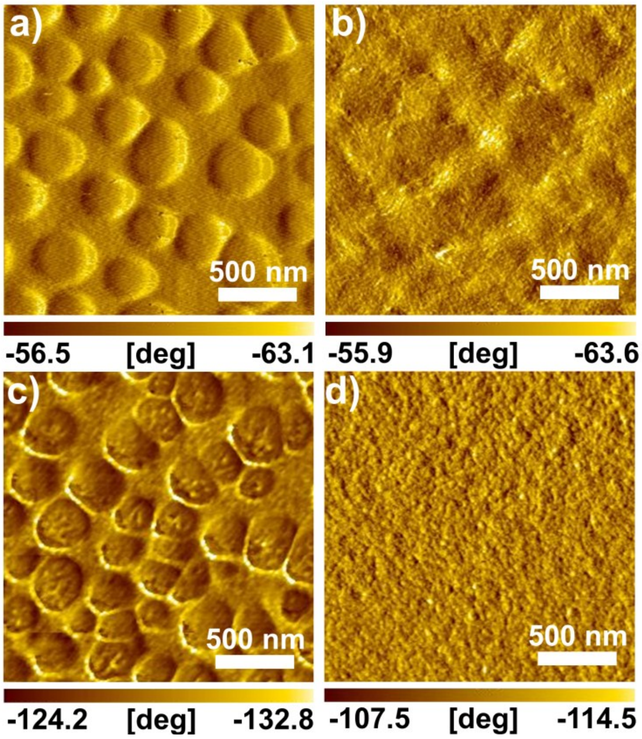

**Fig. S10** AFM phase images of the active layers based on the blends of P-Alkyl:PC$_{71}$BM a) without DIO b) with DIO and P-OEG:PC$_{71}$BM c) without and d) with DIO.

AFM images indicate that the active layers of P-OEG shows more finely mixed phase separation morphology compared to that of P-Alkyl. These can be attributed to the large surface energy of the polymer with OEG side chains, which lead to good miscibility with PC$_{71}$BM and consequently give well mixed phase separation morphology. The phase separation morphology also affect the PSC device performance of the polymers.

**Surface Energy Measurement.** The surface energy of the polymers was characterized and calculated by the contact angles of the two probe liquids (water and glycol) with the Owens and Wendt equation:

$$(1 + \cos\theta)\gamma_{\mathrm{pl}} = 2\left(\gamma_{\mathrm{s}}^{\mathrm{d}}\gamma_{\mathrm{pl}}^{\mathrm{d}}\right)^{1/2} + 2\left(\gamma_{\mathrm{s}}^{\mathrm{p}}\gamma_{\mathrm{pl}}^{\mathrm{p}}\right)^{1/2}$$

where $\gamma_s$ and $\gamma_{pl}$ are the surface energy of the sample and the probe liquid, respectively. The superscripts d and p refer to the dispersion and polar components of the surface energy, respectively.

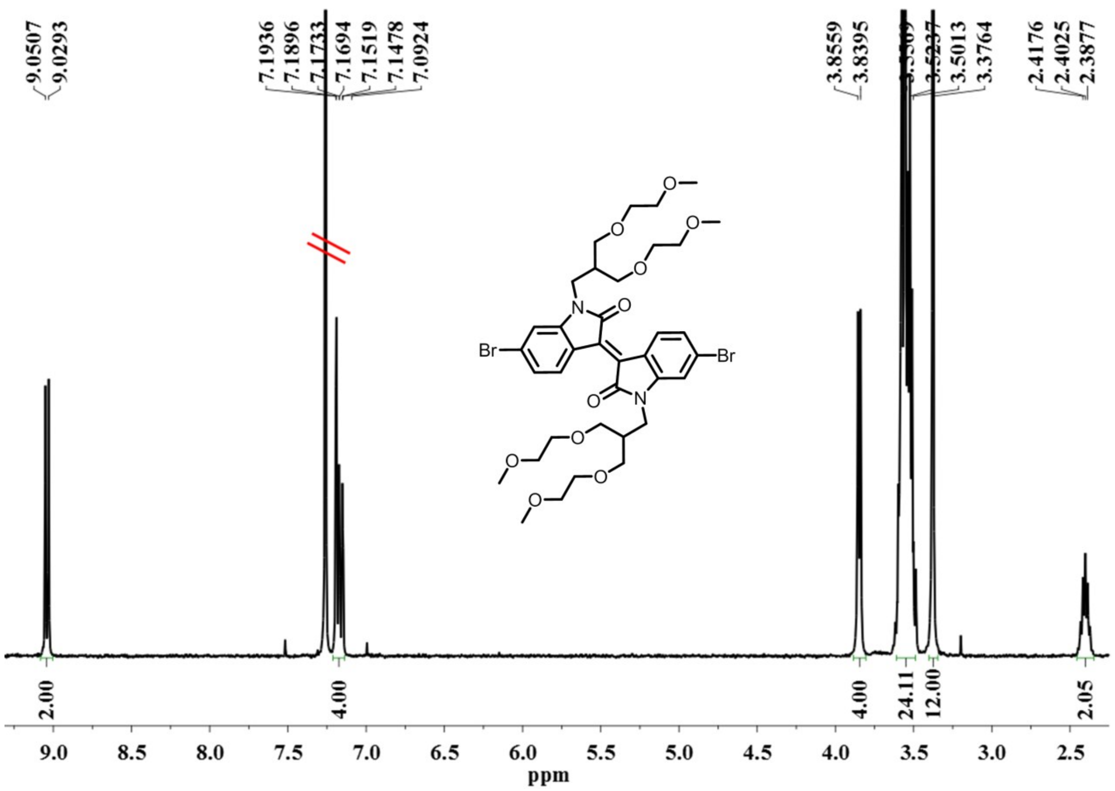

**Fig. S11** $^1$H NMR spectrum of monomer 3.

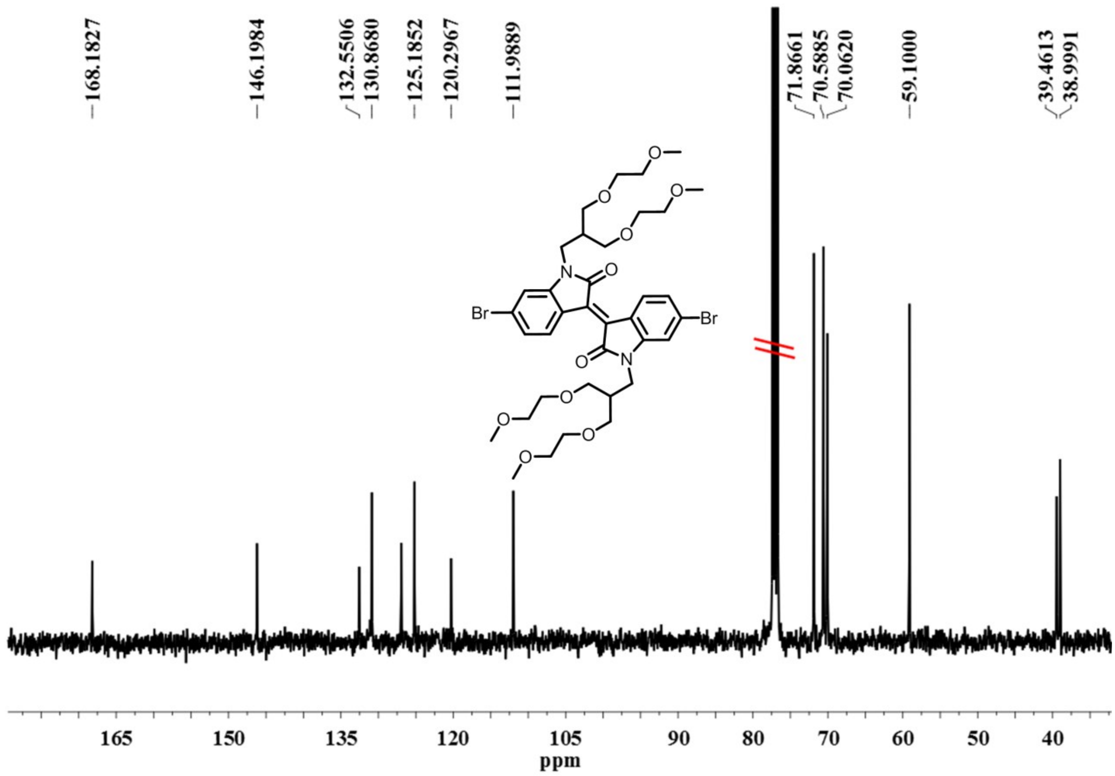

**Fig. S12** $^{13}$C NMR spectrum of monomer 3.

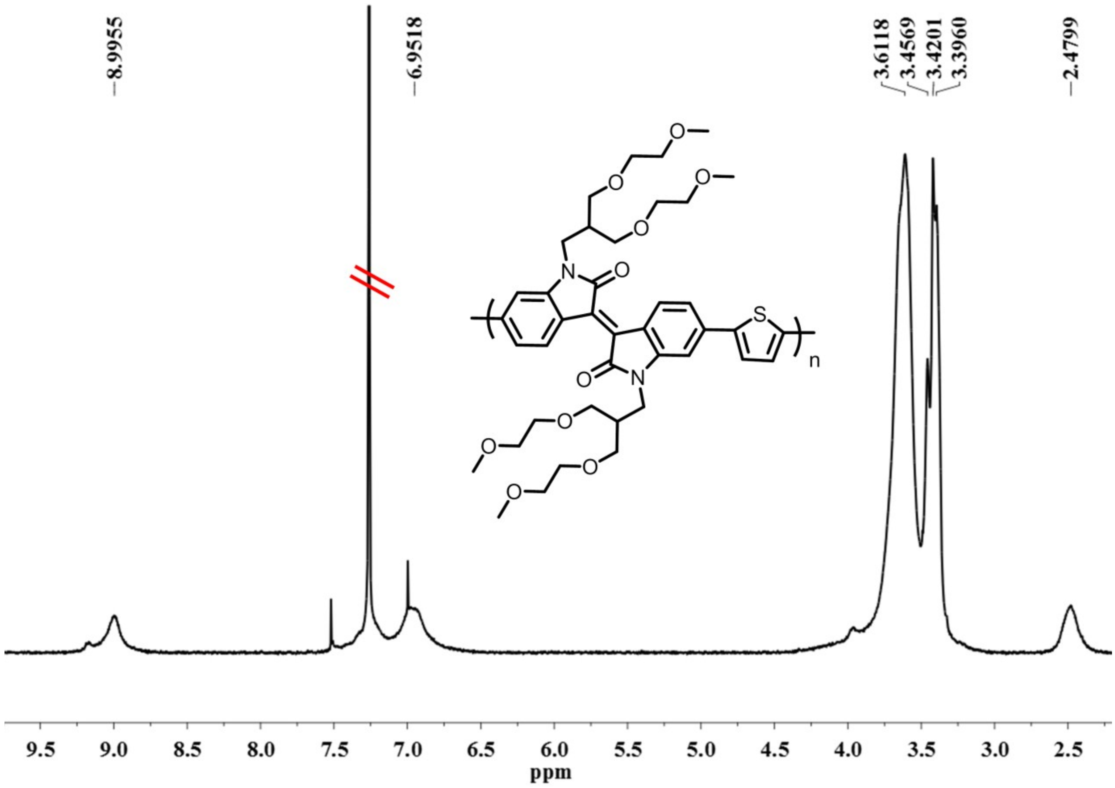

**Fig. S13** $^1$H NMR spectrum of P-OEG.